

## Amyloid- $\beta$ Binds $\text{Cu}^{2+}$ in a Mononuclear Metal Ion Binding Site

Jesse W. Karr, Lauren J. Kaupp,<sup>†</sup> and Veronika A. Szalai\*

Contribution from the Department of Chemistry & Biochemistry, University of Maryland, Baltimore County, 1000 Hilltop Circle, Baltimore, Maryland 21250

Received March 2, 2004; E-mail: vszalai@umbc.edu

**Abstract:** Amyloid- $\beta$  ( $A\beta$ ) peptide is the principal constituent of plaques associated with Alzheimer's disease and is thought to be responsible for the neurotoxicity associated with the disease. Metal ions have been hypothesized to play a role in the formation and neurotoxicity of aggregates associated with Alzheimer's disease (Bush, A. I.; et al. *Proc. Natl. Acad. Sci. U.S.A.* **2003**, *100*, 11934). Elucidation of the chemistry through which transition-metal ions participate in the assembly and toxicity of  $A\beta$  oligomers is important to drug design efforts if inhibition of  $A\beta$  containing bound metal ions becomes a treatment for Alzheimer's disease. In this paper, we report electron paramagnetic resonance (EPR) spectroscopic characterization of  $\text{Cu}^{2+}$  bound to soluble and fibrillar  $A\beta$ . Addition of stoichiometric amounts of  $\text{Cu}^{2+}$  to soluble  $A\beta$  produces an EPR signal at 10 K with observable  $\text{Cu}^{2+}$  hyperfine lines. A nearly identical spectrum is observed for  $A\beta$  fibrils assembled in the presence of  $\text{Cu}^{2+}$ . The EPR parameters are consistent with a Type 2  $\text{Cu}^{2+}$  center with three nitrogen donor atoms and one oxygen donor atom in the coordination sphere of  $\text{Cu}^{2+}$ :  $g_{\parallel} = 2.26$  and  $A_{\parallel} = 174 \pm 4$  G for soluble  $A\beta$  with  $\text{Cu}^{2+}$ , and  $g_{\parallel} = 2.26$  and  $A_{\parallel} = 175 \pm 1$  G for  $A\beta$  fibrils assembled with  $\text{Cu}^{2+}$ . Investigation of the temperature dependence of the EPR signal for  $\text{Cu}^{2+}$  bound to soluble  $A\beta$  or  $\text{Cu}^{2+}$  in fibrillar  $A\beta$  shows that the  $\text{Cu}^{2+}$  center displays normal Curie behavior, indicating that the site is a mononuclear  $\text{Cu}^{2+}$  site. Fibrils assembled in the presence of  $\text{Cu}^{2+}$  contain one  $\text{Cu}^{2+}$  ion per peptide. These results show that the ligand donor atom set to  $\text{Cu}^{2+}$  does not change during organization of  $A\beta$  monomers into fibrils and that neither soluble nor fibrillar forms of  $A\beta(1-40)$  with  $\text{Cu}^{2+}$  contain antiferromagnetically exchange-coupled binuclear  $\text{Cu}^{2+}$  sites in which two  $\text{Cu}^{2+}$  ions are bridged by an intervening ligand.

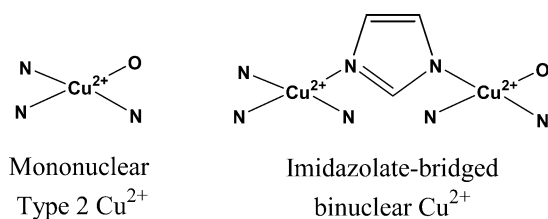
A central, unresolved question in the pathophysiology of Alzheimer's disease (AD) relates to the role of metal ions in plaque formation and neurodegeneration. AD plaques, containing fibrils composed of the 39–42-residue amyloid- $\beta$  ( $A\beta$ ) peptide, are thought to be linked to neurodegeneration in AD.<sup>1</sup> Metal ions have been proposed to play a significant role in the assembly and neurotoxicity of AD fibrils.<sup>2,3</sup> Transition-metal ions can contribute to the neuropathology associated with  $A\beta$  fibrils by affecting the rate of fibril formation,<sup>2-4</sup> by modifying fibril morphology,<sup>5,6</sup> and by direct chemical reaction with  $A\beta$ .<sup>7-9</sup>

Administration of a metal ion chelator decreases deposition of  $A\beta$  in the brains of transgenic mice<sup>10</sup> and releases soluble  $A\beta$  from preformed amyloid deposits,<sup>11</sup> supporting the hypothesis that metal ions are incorporated in AD plaque architecture in vivo. Advances in selective chelation therapy to combat AD<sup>12</sup> require that details of the binding sites of relevant metal ions be known and that the mechanism through which metal ions participate in fibrillization events be better understood.

In vitro study of  $A\beta$  with  $\text{Cu}^{2+}$  and  $\text{Zn}^{2+}$  continues to be used as a model for the role of metals in fibril formation in vivo.<sup>5-7,13,14</sup> The  $\text{Cu}^{2+}$  coordination environment in  $A\beta$  has been

<sup>†</sup> Department of Oceanography, Marine Sciences Building, University of Hawaii at Manoa, 1000 Pope Rd., Honolulu, HI 96822.

- (1) Jacobson, D. R.; Buxbaum, J. N. *Adv. Hum. Genet.* **1991**, *20*, 69. Sipe, J. D. *Annu. Rev. Biochem.* **1992**, *61*, 947.
- (2) Bush, A. I.; Multhaup, G.; Moir, R. D.; Williamson, T. G.; Small, D. H.; Rumble, B.; Pollwein, P.; Beyreuther, K.; Masters, C. L. *J. Biol. Chem.* **1993**, *268*, 16109. Rottkamp, C. A.; Raina, A. K.; Zhu, X.; Gaier, E.; Bush, A. I.; Atwood, C. S.; Chevion, M.; Perry, G.; Smith, M. A. *Free Radical Biol. Med.* **2001**, *30*, 447.
- (3) Bush, A. I.; Pettingell, W. H.; Multhaup, G.; Paradis, M. D.; Vonsattel, J. P.; Gusella, J. F.; Beyreuther, K.; Masters, C. L.; Tanzi, R. E. *Science* **1994**, *265*, 1464.
- (4) Burkoth, T. S.; Benzinger, T. L. S.; Urban, V.; Morgan, D. M.; Gregory, D. M.; Thiagarajan, P.; Botta, R. E.; Meredith, S. C.; Lynn, D. G. *J. Am. Chem. Soc.* **2000**, *122*, 7883. Cuajungco, M. P.; Goldstein, L. E.; Nunomura, K.; Smith, M. A.; Lim, J. T.; Atwood, C. S.; Huang, X.; Farrag, Y. W.; Perry, G.; Bush, A. I. *J. Biol. Chem.* **2000**, *275*, 19439.
- (5) Morgan, D. M.; Dong, J.; Jacob, J.; Lu, K.; Apkarian, R. P.; Thiagarajan, P.; Lynn, D. G. *J. Am. Chem. Soc.* **2002**, *124*, 12544.
- (6) Zou, J.; Kajita, K.; Sugimoto, N. *Angew. Chem., Int. Ed.* **2001**, *40*, 2274.
- (7) Curtain, C. C.; Ali, F.; Volitakis, I.; Cherny, R. A.; Norton, R. S.; Beyreuther, K.; Barrow, C. J.; Masters, C. L.; Bush, A. I.; Barnham, K. J. *J. Biol. Chem.* **2001**, *276*, 20466.
- (8) Huang, X.; Cuajungco, M. P.; Atwood, C. G.; Hartshorn, M. A.; Tyndall, J. D. A.; Hanson, G. R.; Stokes, K. C.; Leopold, M.; Multhaup, G.; Goldstein, L. E.; Scarpa, R. C.; Saunders, A. J.; Lim, J.; Moir, R. D.; Glabe, C.; Bowden, E. F.; Masters, C. L.; Fairlie, D. P.; Tanzi, R. E.; Bush, A. I. *J. Biol. Chem.* **1999**, *274*, 37111.
- (9) Huang, X.; Atwood, C. G.; Hartshorn, M. A.; Multhaup, G.; Goldstein, L. E.; Scarpa, R. C.; Cuajungco, M. P.; Gray, D. N.; Lim, J.; Moir, R. D.; Tanzi, R. E.; Bush, A. I. *Biochemistry* **1999**, *38*, 7609.
- (10) Cherny, R. A.; Atwood, C. S.; Xilinas, M. E.; Gray, D. N.; Jones, W. D.; McLean, C. A.; Barnham, K. J.; Volitakis, I.; Fraser, F. W.; Kim, Y.-S.; Huang, X.; Goldstein, L. E.; Moir, R. D.; Lim, J. T.; Beyreuther, K.; Zheng, H.; Tanzi, R. E.; Masters, C. L.; Bush, A. I. *Neuron* **2001**, *30*, 665.
- (11) Cherny, R. A.; Legg, J. T.; McLean, C. A.; Fairlie, D. P.; Huang, X.; Atwood, C. S.; Beyreuther, K.; Tanzi, R. E.; Masters, C. L.; Bush, A. I. *J. Biol. Chem.* **1999**, *274*, 23223.
- (12) Bush, A. I.; Tanzi, R. E. *Proc. Natl. Acad. Sci. U.S.A.* **2002**, *99*, 7317.

**Chart 1.** Mononuclear and Binuclear  $\text{Cu}^{2+}$  Ion Sites<sup>a</sup>

<sup>a</sup>The mononuclear  $\text{Cu}^{2+}$  site has three nitrogen donor atoms and one oxygen donor atom (3N1O). A binuclear  $\text{Cu}^{2+}$  site could form when the oxygen atom donor on one  $\text{Cu}^{2+}$  is replaced by a deprotonated histidine residue, which bridges two  $\text{Cu}^{2+}$  ions.<sup>7</sup>

probed by Raman and electron paramagnetic resonance (EPR) spectroscopies.<sup>8,15</sup> EPR spectroscopy is an accepted method for determining the ligand donor atom identities for  $\text{Cu}^{2+}$  sites through measurement of the magnitude of the  $\text{Cu}^{2+}$  hyperfine coupling constant,  $A_{\parallel}$ , and the corresponding  $g$  value,  $g_{\parallel}$ .<sup>16</sup> When 1 equiv of  $\text{Cu}^{2+}$  is added to soluble  $A\beta(1-40)$ , the  $\text{Cu}^{2+}$  EPR spectrum indicates that three nitrogen donor ligands and one oxygen donor ligand (3N1O) are in the  $\text{Cu}^{2+}$  coordination sphere.<sup>8</sup> Additional EPR spectroscopic studies of  $\text{Cu}^{2+}$  with soluble  $A\beta(1-28)$ , a shortened version of  $A\beta(1-40)$  that also forms aggregates, suggest the existence of multiple soluble copper-peptide species as a function of the  $\text{Cu}^{2+}$ :peptide ratio.<sup>7</sup> In contrast to the EPR results, Raman measurements of  $\text{Cu}^{2+}$  bound to soluble  $A\beta$  suggest that the  $\text{Cu}^{2+}$  ligands are histidine and deprotonated amides.<sup>15</sup> Characteristic Raman bands for  $\text{Cu}^{2+}$  bound to histidine were observed for aggregates of  $A\beta(1-40)$  assembled in the presence of  $\text{Cu}^{2+}$ , suggesting that  $\text{Cu}^{2+}$  cross-links  $\beta$ -sheets via histidines from multiple peptides. Together, these data indicate that  $A\beta$  oligomers containing histidine-bridged  $\text{Cu}^{2+}$  centers are possible precursors to metal-cross-linked  $\beta$ -sheets.<sup>5</sup> A binuclear imidazolate-bridged  $\text{Cu}^{2+}$  site (Chart 1), similar to that found in copper, zinc superoxide dismutase (Cu,Zn-SOD), has been proposed as a possible structure for soluble  $A\beta(1-28)$  in the presence of stoichiometric amounts of  $\text{Cu}^{2+}$ .<sup>7</sup> Controversy about the coordination environment of  $\text{Cu}^{2+}$  in soluble vs fibrillar forms of  $A\beta$  requires that further work be undertaken to firmly establish the  $\text{Cu}^{2+}$  coordination environment in  $A\beta$ .

We have used low-temperature EPR spectroscopy to determine the ligand donor atoms to  $\text{Cu}^{2+}$  in fibrillar  $A\beta(1-40)$ . Electron microscopy images show that our samples, assembled from  $A\beta(1-40)$  in the presence of  $\text{Cu}^{2+}$ , are  $A\beta$  fibrils. By inductively coupled plasma mass spectrometry (ICP-MS) and amino acid analysis, 1.1  $\text{Cu}^{2+}$  ions bind per  $A\beta(1-40)$  peptide in our fibrils. The Curie temperature dependence of the EPR signal for  $\text{Cu}^{2+}$  bound to  $A\beta(1-40)$  in both soluble and fibrillar forms is consistent with  $\text{Cu}^{2+}$  in a mononuclear metal ion binding site in the peptide.

## Materials and Methods

Commercially available  $A\beta(1-40)$  peptide was obtained from rPeptide (Athens, GA) or Bachem (King of Prussia, PA). Biological

grade glycerol, Tris, and sodium chloride were purchased from Fisher. Quartz EPR tubes (4 mm o.d.) were purchased from Wilmad (Buena, NJ). Solutions were prepared in MilliQ water (resistivity >18 m $\Omega$ , total organic content <35 ppb).

**Sample Preparation.** Peptide was monomerized with hexafluoro-2-propanol (HFIP) according to literature procedures and stored at  $-80^{\circ}\text{C}$  in HFIP.<sup>17</sup> The peptide in HFIP was removed with a Hamilton gastight syringe that had been washed with multiple volumes of HFIP. Immediately prior to use of peptide, HFIP was removed using a spin-vacuum system. Preparation of samples by dissolution in HFIP followed by removal of HFIP produces homogeneous solutions of monomeric peptide.<sup>18</sup>

Samples of soluble  $A\beta(1-40)$  were made by dissolving dried peptide in buffer containing 100 mM Tris, 150 mM NaCl, pH 7.4, with 50% glycerol (v/v). Inclusion of glycerol as a cryoprotectant for biological samples is an accepted method for protecting sample fidelity.<sup>19,20</sup> We have attempted to use lower concentrations of glycerol in our samples, but find that the samples do not make good glasses, a prerequisite for EPR spectral collection at low temperatures. After the peptide was resuspended in buffer, an aliquot of the sample was removed for peptide concentration determination. The appropriate concentration of a  $\text{Cu}^{2+}$  stock solution in buffer was added to the remainder of the peptide sample. The sample was vortexed, transferred to a quartz EPR tube,<sup>7,8</sup> and frozen to 77 K prior to data collection. The time between addition of  $\text{Cu}^{2+}$  to the peptide and freezing of the sample is not sufficient to generate a substantial concentration of  $\beta$ -sheets as detected by thioflavin T fluorescence assay.<sup>21</sup>

For fibrillar samples, the peptide as prepared above was incubated at  $37^{\circ}\text{C}$  for 7–14 days without agitation in the presence of  $\text{Cu}^{2+}$ . Samples were then assayed for fibril formation by transmission electron microscopy and thioflavin T fluorescence. Fibrils for EPR experiments were formed in 100 mM Tris, 150 mM NaCl, pH 7.4, with (Figures 2 and 3) or without (Figure 4) 50% glycerol (v/v), separated by centrifugation (30 min, 16000 rcf), washed once with 100  $\mu\text{L}$  of buffer containing 50% glycerol (v/v), and resuspended in 100  $\mu\text{L}$  of the same buffer. Fibrils for ICP-MS experiments were formed in 100 mM Tris, 150 mM NaCl, pH 7.4, separated by centrifugation, washed with 20  $\mu\text{L}$  of water to remove salts, and then dried in a spin-vacuum system. ICP-MS was performed by the ICP-HEX-MS Laboratory in the Department of Geological Sciences at Michigan State University.<sup>22</sup>

Peptide concentrations were determined on the basis of the absorbance at 214 nm using a calibration curve generated with BSA standards from Sigma. The concentration of peptide in the stock solution also was measured by amino acid analysis (AAA Service Laboratory, Inc., Portland, OR). Amino acid analysis of fibrils without  $\text{Cu}^{2+}$ , but assembled from the same peptide stock solution used to prepare fibrils with  $\text{Cu}^{2+}$ , also was performed (AAA Service Laboratory, Inc.).<sup>22</sup>

The <sup>63,65</sup> $\text{Cu}^{2+}$  stock solution was generated by dissolution of cleaned copper wire in nitric acid and water. The  $\text{Cu}^{2+}$  concentrations for samples in 100 mM Tris, 150 mM NaCl, pH 7.4, with 50% glycerol (v/v) were determined on the basis of a calibration curve generated from  $\text{Cu}^{2+}$  standards in the same buffer. The concentration of  $\text{Cu}^{2+}$  in the  $\text{Cu}^{2+}$  EPR standards was assayed by chelation with bath-

- (13) Atwood, C. S.; Scarpa, R. C.; Huang, X.; Moir, R. D.; Jones, W. D.; Fairlie, D. P.; Tanzi, R. E.; Bush, A. I. *J. Neurochem.* **2000**, *75*, 1219.  
 (14) Jobling, M. F.; Huang, X.; Stewart, L. R.; Barnham, K. J.; Curtain, C.; Volitakis, I.; Perugini, M.; White, A. R.; Cherny, R. A.; Masters, C. L.; Barrow, C. J.; Collins, S. J.; Bush, A. I.; Cappai, R. *Biochemistry* **2001**, *40*, 8073.  
 (15) Miura, T.; Suzuki, K.; Kohata, N.; Takeuchi, H. *Biochemistry* **2000**, *39*, 7024.  
 (16) Peisach, J.; Blumberg, W. E. *Arch. Biochem. Biophys.* **1974**, *165*, 691.

- (17) Wood, S. J.; Maleeff, B.; Hart, T.; Wetzel, R. *J. Mol. Biol.* **1996**, *256*, 870.  
 (18) Stine, W. B., Jr.; Dahlgren, K. N.; Krafft, G. A.; LaDu, M. J. *J. Biol. Chem.* **2003**, *278*, 11612.  
 (19) Aronoff-Spencer, E.; Burns, C. S.; Avdievich, N. I.; Gerfen, G. J.; Peisach, J.; Antholine, W. E.; Ball, H. L.; Cohen, F. E.; Prusiner, S. B.; Millhauser, G. L. *Biochemistry* **2000**, *39*, 13760.  
 (20) Wertz, J. E.; Bolton, J. R. *Electron Spin Resonance: Elementary Theory and Practical Applications*; Chapman & Hall: New York, 1972.  
 (21) Levine, H. I. *Methods Enzymol.* **1999**, *309*, 274.  
 (22) The  $\text{Cu}^{2+}$  concentration determined by ICP-MS for fibrils assembled in the presence of  $\text{Cu}^{2+}$  was  $750 \pm 75$  ppb in 1 mL. By amino acid analysis, the concentrations of peptide determined for three injections of a 100  $\mu\text{L}$  initial volume sample of fibrils were 105.17, 106.55, and 107.47  $\mu\text{M}$ . The  $\text{Cu}^{2+}$  to peptide ratio is an estimate because standard amino acid analysis equipment is incompatible with high concentrations of metal ions.

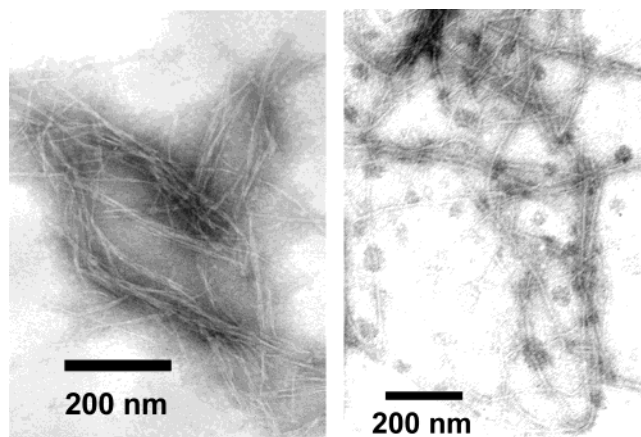


**Figure 1.** Negatively stained TEM images of aged solutions of A $\beta$ (1–40) containing Cu $^{2+}$ . Samples were prepared as described in the Materials and Methods and stained with 1% phosphotungstic acid (left) or 1% uranyl acetate (right). The magnification is 25000 $\times$ .

ocuproinedisulfonic acid (BC) and reduction with ascorbate.<sup>23</sup> The quantity of total copper as [Cu(BC) $_2$ ] $^{3-}$  was quantified using  $\epsilon_{483} = 12500 \text{ M}^{-1} \text{ cm}^{-1}$ .<sup>23</sup> The 0, 25, and 100  $\mu\text{M}$  Cu $^{2+}$  standards contained  $0.0 \pm 0.7$ ,  $26.9 \pm 0.6$ , and  $108.4 \pm 0.6 \mu\text{M}$  Cu $^{2+}$ , respectively.

**Electron Microscopy.** Electron microscopy images were collected at the University of Maryland, Baltimore Dental School with a JEOL JEMEX II transmission electron microscope. Samples were placed on 300-mesh Formvar films and stained with 1% phosphotungstic acid or 1% uranyl acetate.

**EPR Spectroscopy.** EPR spectra were collected on a Bruker EMX 6/1 spectrometer equipped with a frequency meter and an Oxford Instruments ESR900 liquid He cryostat system. Spectral collection parameters are given in the figure captions. Errors given for the peak widths at half-height are based on relative errors for the peak heights. Relative errors were calculated by dividing the average noise height in each spectrum by the measured peak height. Errors for the doubly integrated spectra were calculated from the maximum variation in peak height as a function of field position.

## Results and Discussion

**Characterization of A $\beta$ (1–40) Fibrils Assembled in the Presence of Cu $^{2+}$ .** In our experiments, the pH of the buffers promotes the formation of fibrils over the formation of amorphous aggregates.<sup>17</sup> Electron microscopy clearly shows the presence of protofilaments and fibrils in aged solutions of A $\beta$ (1–40) peptide with Cu $^{2+}$  (Figure 1). The width of the protofilaments is  $6 \pm 1 \text{ nm}$ , which is similar to the width of protofilaments assembled in the absence of Cu $^{2+}$ .<sup>24,25</sup> No amorphous aggregates were observed, confirming that EPR spectra of aggregates isolated by centrifugation and resuspended in buffer are of fibrils that contain Cu $^{2+}$ .

To determine the Cu $^{2+}$  to peptide ratio in fibrils, ICP-MS and amino acid analyses were performed on matched samples. By ICP-MS, fibrils assembled with Cu $^{2+}$  contained  $0.0118 \pm 0.0013 \mu\text{mol}$  of Cu $^{2+}$ . By amino acid analysis, fibrils contained  $0.0106 \pm 0.0001 \mu\text{mol}$  of peptide, giving an estimated ratio of 1.1 mol of Cu $^{2+}$ /mol of peptide.<sup>22</sup> This result is consistent with the 1:1 stoichiometry for Cu $^{2+}$  bound to soluble A $\beta$  published by Garzon-Rodriguez et al.<sup>26</sup> Other Cu $^{2+}$  to peptide ratios have

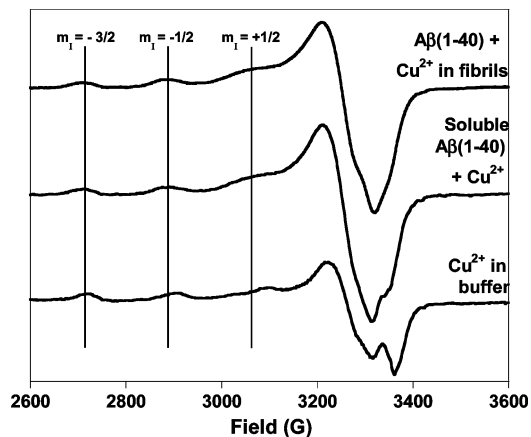


**Figure 2.** EPR spectra of Cu $^{2+}$  in A $\beta$ (1–40) fibrils, Cu $^{2+}$  with soluble A $\beta$ (1–40), or 25  $\mu\text{M}$  Cu $^{2+}$  in buffer. Hyperfine lines arising from the  $I = 3/2$   $^{63,65}\text{Cu}$  nucleus are identified by the  $m_I$  value. A $\beta$ (1–40) fibrils (37  $\mu\text{M}$  initial peptide concentration) were assembled in the presence of 48  $\mu\text{M}$  Cu $^{2+}$ , separated by centrifugation, and washed to remove excess Cu $^{2+}$ ;  $g_{\parallel} = 2.26$ ,  $A_{\parallel} = 175 \pm 1 \text{ G}$ . Soluble A $\beta$ (1–40) with Cu $^{2+}$  contains 50  $\mu\text{M}$  A $\beta$  and 50  $\mu\text{M}$  Cu $^{2+}$ ;  $g_{\parallel} = 2.26$ ,  $A_{\parallel} = 174 \pm 4 \text{ G}$ . All samples are in 100 mM Tris, 150 mM NaCl, pH 7.4, buffer with 50% glycerol (v/v). EPR conditions:  $T = 10 \text{ K}$ ; modulation amplitude 10 G; power 0.5 mW; gain  $5 \times 10^4$ ; frequency 9.38 GHz; time constant 40.96 ms; conversion time 40.96 ms; four or eight scans.

been reported: approximately two Cu $^{2+}$  ions per precipitated A $\beta$ (1–40) and essentially none per soluble peptide.<sup>13</sup> These stoichiometries were determined by UV–vis spectrophotometric detection of soluble peptide (Micro BCA assay) and metal ions.<sup>13</sup> The ratio obtained by ICP-MS and amino acid analysis reported here is derived from direct measurements on fibrils. A possible explanation for the discrepancies in Cu $^{2+}$ :peptide ratios could be the existence of multiple types of peptide precipitates, a common occurrence with amyloid peptides.<sup>17,18,27</sup> In our case, EM confirms that the solid samples assayed by ICP-MS and amino acid analysis are A $\beta$  fibrils.

**Spectroscopic Measurements on Cu $^{2+}$  Bound to A $\beta$ (1–40).** The coordination environment of Cu $^{2+}$  in soluble or fibrillar forms of A $\beta$  was monitored by EPR spectroscopy. EPR spectra collected at 10 K of soluble A $\beta$ (1–40) with stoichiometric amounts of Cu $^{2+}$  show Cu $^{2+}$  EPR spectra with distinguishable hyperfine lines arising from the  $^{63,65}\text{Cu}^{2+}$   $I = 3/2$  nucleus ( $m_I$  labels in Figure 2). The magnitudes of the  $A_{\parallel}$  and  $g_{\parallel}$  values are consistent with a Type 2 Cu $^{2+}$  center with mostly nitrogen donor atoms (Figure 2).<sup>16</sup> Our results are in agreement with the previously proposed 3N1O coordination environment for Cu $^{2+}$  bound to soluble A $\beta$ (1–40).<sup>8</sup> The major differences in the EPR spectra for a Cu $^{2+}$  center ligated to four N donor atoms rather than 3N1O coordination are in the magnitudes of the  $A_{\parallel}$  and  $g_{\parallel}$  values. On average,  $A_{\parallel}$  values are slightly higher and  $g_{\parallel}$  is slightly lower for 4N coordination than for 3N1O coordination.<sup>16</sup> When fibrils assembled in the presence of Cu $^{2+}$  and glycerol are separated by centrifugation and washed with buffer that does not contain Cu $^{2+}$ , the EPR spectrum of Cu $^{2+}$  bound to fibrils is nearly identical to that observed for Cu $^{2+}$  with soluble A $\beta$ (1–40). The major difference between the spectra for the soluble and fibrillar forms of A $\beta$ (1–40) containing Cu $^{2+}$  is in the  $g_{\perp}$  region of the spectrum. This region of the spectrum is sensitive to the sequence order of ligand donor atoms. Thus, even when the donor atom composition is 3N1O in both samples,  $g_{\perp}$  varies

(23) Moffett, J.; Zika, R. G.; Petasne, R. G. *Anal. Chim. Acta* **1985**, *175*, 171.

(24) Harper, J. D.; Wong, S. S.; Lieber, C. M.; Lansbury, P. T., Jr. *Biochemistry* **1999**, *38*, 8972.

(25) Tycko, R. *Curr. Opin. Struct. Biol.* **2004**, *14*, 96.

(26) Garzon-Rodriguez, W.; Yatsimirsky, A. K.; Glabe, C. G. *Bioorg. Med. Chem. Lett.* **1999**, *9*, 2243.

(27) Rochet, J.-C.; Lansbury, P. T., Jr. *Curr. Opin. Struct. Biol.* **2000**, *20*, 60.

depending on where a nitrogen atom donor such as histidine appears in the sequence.<sup>28</sup>

Our results show that the ligand donor atom set for  $\text{Cu}^{2+}$  does not change whether  $\text{Cu}^{2+}$  is bound to soluble  $A\beta$  or incorporated into  $A\beta$  fibrils. The  $g_{\parallel}$  and  $A_{\parallel}$  values for  $\text{Cu}^{2+}$  bound to soluble or fibrillar  $A\beta$  are most consistent with a donor atom set of  $3\text{N}1\text{O}$ .<sup>8,16</sup> These results alone cannot be used to determine the identities of the ligating groups for  $\text{Cu}^{2+}$  bound to soluble and fibrillar  $A\beta(1-40)$ . However, if ligands to  $\text{Cu}^{2+}$  do not change during fibrillogenesis, fibrils assembled in the presence of  $\text{Cu}^{2+}$  could contain distinct structural regions: the N-terminal segment of the peptide could bind  $\text{Cu}^{2+}$ , while the C-terminus could participate in  $\beta$ -sheet formation. This hypothesis is consistent with the demonstration that the N-terminal region of the peptide is not confined rigidly in mature fibrils.<sup>29</sup> The amino acids that have been proposed to bind  $\text{Cu}^{2+}$  in  $A\beta$  are between residues 6 and 14,<sup>7,15,30</sup> suggesting that this region of the peptide might be available to bind metal ions in fibrils without disrupting fibril formation.

Solid-state NMR structural studies on  $A\beta$  fibrils have shown that fibrils contain parallel  $\beta$ -sheets.<sup>25,31</sup> The interstrand distance in the parallel  $\beta$ -sheets is approximately 5 Å.<sup>32</sup> If a parallel  $\beta$ -sheet model holds for fibrils with approximately one  $\text{Cu}^{2+}$  per peptide,  $\text{Cu}^{2+}$  ions could be in close enough proximity in the fibrils to interact via dipolar and/or exchange interactions. Dipolar interaction between paramagnets can cause spectral broadening. The peak widths at half-height for the discernible  $\text{Cu}^{2+}$  hyperfine peaks in soluble  $A\beta(1-40)$  are  $57 \pm 5$  ( $m_l = -3/2$ , Figure 1),  $65 \pm 8$  ( $m_l = -1/2$ ), and  $118 \pm 34$  G ( $m_l = +1/2$ ). In fibrillar  $A\beta(1-40)$ , the corresponding  $\text{Cu}^{2+}$  hyperfine peak widths at half-height are  $58 \pm 5$ ,  $60 \pm 5$ , and  $116 \pm 27$  G. Thus, significant broadening is not apparent in the spectrum of  $\text{Cu}^{2+}$ -containing fibrils in Figure 1. To our knowledge, the peptide orientation in fibrils containing metal ions has not been determined. Therefore, it is possible that the strands in fibrils containing  $\text{Cu}^{2+}$  are oriented in a parallel  $\beta$ -sheet arrangement that does not produce observable dipolar broadening between  $\text{Cu}^{2+}$  ions or that the strands are aligned in a configuration other than a parallel  $\beta$ -sheet. It should be noted that  $A\beta$  fibril structural assignments are not always in agreement, with the exact composition of the peptide playing a major factor in controlling fibril morphology.<sup>33</sup>

If an antiferromagnetically exchange-coupled binuclear  $\text{Cu}^{2+}$  site exists in soluble or fibrillar  $A\beta$ , it should have a diamagnetic ground state. The magnetic ground state of a paramagnetic system can be determined by EPR spectroscopy.<sup>20</sup> The EPR signal intensity is temperature dependent, with the largest

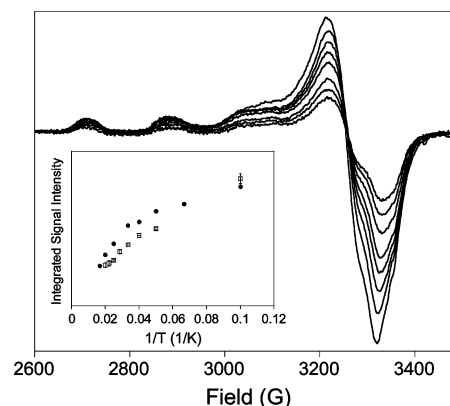


**Figure 3.** Effect of temperature on the EPR spectrum of  $\text{Cu}^{2+}$  in  $A\beta(1-40)$  fibrils. EPR parameters are as in Figure 2 except that  $T = 10-60$  K. Microwave power saturation measurements were collected at all temperatures to ensure that spectral intensities are not decreased through saturation effects. Inset: Curie plot of doubly integrated  $\text{Cu}^{2+}$  EPR spectral intensities for  $\text{Cu}^{2+}$  with soluble  $A\beta(1-40)$  (squares) or  $\text{Cu}^{2+}$  in  $A\beta(1-40)$  fibrils (circles). Samples are the same as in Figure 2.

intensity observed when a single paramagnetic state is fully populated.<sup>20</sup> We detect a spectrum of  $\text{Cu}^{2+}$  bound to  $A\beta$  at temperatures as low as 6 K, indicating that the ground state of  $\text{Cu}^{2+}$  bound to soluble  $A\beta$  or bound to fibrillar  $A\beta$  is paramagnetic. Magnetic susceptibility data for imidazolate-bridged binuclear  $\text{Cu}^{2+}$  model complexes indicate a diamagnetic ground state, so these complexes should not display an EPR signal below 50 K.<sup>34</sup> Antiferromagnetically coupled  $\text{Cu}^{2+}$  ions in  $\text{Cu,Cu-SOD}$  show a 90 K EPR spectrum that is diminished relative to that for  $\text{Cu,Zn-SOD}$  because it arises from the  $S = 1$  excited state.<sup>35</sup> Because an EPR signal for  $\text{Cu}^{2+}$  bound to soluble  $A\beta$  is detectable at temperatures below 60 K and we detect no half-field transition (not shown), exchange-coupled binuclear  $\text{Cu}^{2+}$  centers in  $A\beta$  are unlikely.

To support the interpretation that  $\text{Cu}^{2+}$  bound to  $A\beta$  is a mononuclear  $\text{Cu}^{2+}$  site, the temperature dependence of spectra for  $\text{Cu}^{2+}$ -bound peptide samples was monitored. The spectrum of  $\text{Cu}^{2+}$  bound to  $A\beta(1-40)$  decreases and broadens as the temperature is raised (Figure 3). A Curie plot shows that doubly integrated EPR spectral intensities for  $\text{Cu}^{2+}$  bound to  $A\beta$  fibrils or  $\text{Cu}^{2+}$  bound to soluble  $A\beta$  have Curie temperature dependences, characteristic of mononuclear  $\text{Cu}^{2+}$  (Figure 3, inset). The binuclear imidazolate-bridged  $\text{Cu}^{2+}$  model for 1:1  $\text{Cu}^{2+}/A\beta(1-28)$  complexes is based on experiments performed at pH 7.4 in the presence of  $\text{Cu}^{2+}$ , which are the same conditions under which our experiments were performed.<sup>7</sup>

The spectra in Figure 3 are for fibrils assembled in the presence of glycerol. Glycerol has been shown to affect the rate

(28) Pogni, R.; Baratto, M. C.; Busi, E.; Basosi, R. *J. Inorg. Biochem.* **1999**, *73*, 157.

(29) Iwata, K.; Eyles, S. J.; Lee, J. P. *J. Am. Chem. Soc.* **2001**, *123*, 6728. Khetarpal, I.; Williams, A.; Murphy, C.; Bledsoe, B.; Wetzel, R. *Biochemistry* **2001**, *40*, 11757. Roher, A. E.; Baudry, J.; Chaney, M. O.; Kuo, Y. M.; Stine, W. B.; Emmerling, M. R. *Biochim. Biophys. Acta* **2000**, *1502*, 31. Wang, S. S.-S.; Tobler, S. A.; Good, T. A.; Fernandez, E. J. *Biochemistry* **2003**, *42*, 9507.

(30) Liu, S.-T.; Howlett, G.; Barrow, C. J. *Biochemistry* **1999**, *38*, 9373.

(31) Balbach, J. J.; Petkova, A. T.; Oyler, N. A.; Antzutkin, O. N.; Gordon, D. J.; Meredith, S. C.; Tycko, R. *Biophys. J.* **2002**, *83*, 1205. Benzinger, T. L. S.; Gregory, D. M.; Burkoth, T. S.; Miller-Auer, H.; Lynn, D. G.; Botto, R. E.; Meredith, S. C. *Proc. Natl. Acad. Sci. U.S.A.* **1998**, *95*, 13407. Benzinger, T. L. S.; Gregory, D. M.; Burkoth, T. S.; Miller-Auer, H.; Lynn, D. G.; Botto, R. E.; Meredith, S. C. *Biochemistry* **2000**, *39*, 3491. Antzutkin, O. N.; Leapman, R. D.; Balbach, J. J.; Tycko, R. *Biochemistry* **2002**, *41*, 15436.

(32) Kirschner, D. A.; Abraham, C.; Selkoe, D. J. *Proc. Natl. Acad. Sci. U.S.A.* **1986**, *83*, 503.

(33) Costa, P. R.; Kocisko, D. A.; Sun, B. Q.; Lansbury, P. T., Jr.; Griffin, R. G. *J. Am. Chem. Soc.* **1997**, *119*, 10487. Balbach, J. J.; Ishii, Y.; Antzutkin, O. N.; Leapman, R. D.; Rizzo, N. W.; Dyda, F.; Reed, J.; Tycko, R. *Biochemistry* **2000**, *39*, 13748. Petkova, A. T.; Buntkowsky, G.; Dyda, F.; Leapman, R. D.; Yau, W. M.; Tycko, R. *J. Mol. Biol.* **2004**, *335*, 247. Gordon, D. J.; Balbach, J. J.; Tycko, R.; Meredith, S. C. *Biophys. J.* **2004**, *86*, 428. Hou, L.; Shao, H.; Zhang, Y.; Li, H.; Menon, N. K.; Neuhaus, E. B.; Brewer, J. M.; Byeon, I. J.; Ray, D. G.; Vitek, M. P.; Iwashita, T.; Makula, R. A.; Przybyla, A. B.; Zagorski, M. G. *J. Am. Chem. Soc.* **2004**, *126*, 1992.

(34) Li, D.; Li, S.; Yang, D.; Yu, J.; Huang, J.; Li, Y.; Tang, W. *Inorg. Chem.* **2003**, *42*, 6071. Ohtsu, H.; Shimazaki, Y.; Odani, A.; Yamauchi, O.; Mori, W.; Itoh, S.; Fukuzumi, S. *J. Am. Chem. Soc.* **2000**, *122*, 5733.

(35) Lu, Y.; LaCroix, L. B.; Lowery, M. D.; Solomon, E. I.; Bender, C. J.; Peisach, J.; Roe, J. A.; Gralla, E. B.; Valentine, J. S. *J. Am. Chem. Soc.* **1993**, *115*, 5907. Lu, Y.; Roe, J. A.; Bender, C. J.; Peisach, J.; Banci, L.; Bertini, I.; Gralla, E. B.; Valentine, J. S. *Inorg. Chem.* **1996**, *35*, 2.

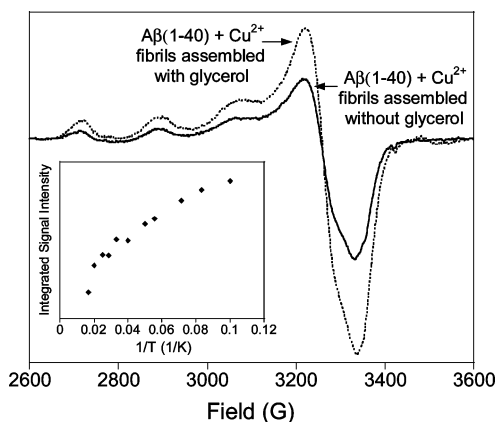


**Figure 4.** EPR spectra of  $\text{Cu}^{2+}$  in  $\text{A}\beta(1-40)$  fibrils assembled in buffer with (dashed line) or without (solid line) glycerol. Both sets of fibrils were separated by centrifugation, washed with the appropriate buffer (100 mM Tris, 150 mM NaCl, pH 7.4, buffer with or without 50% glycerol (v/v)), and resuspended in buffer containing 50% glycerol (v/v) immediately prior to data collection. The spectra have different overall intensities because the amount of fibrils collected differs between samples. EPR conditions:  $T = 20$  K; modulation amplitude 10 G; power 0.5 mW; gain  $5 \times 10^4$ ; frequency 9.38 GHz; time constant 40.96 ms; conversion time 40.96 ms; eight scans. Inset: Curie plot of doubly integrated  $\text{Cu}^{2+}$  EPR spectral intensities for  $\text{Cu}^{2+}$ -containing  $\text{A}\beta(1-40)$  fibrils assembled without glycerol. EPR parameters are as above except that  $T = 10-60$  K.

of fibril formation.<sup>36</sup> In this work, the rate of fibril formation in the presence of  $\text{Cu}^{2+}$  was not monitored; spectra were collected of soluble peptide containing  $\text{Cu}^{2+}$  (the initial time point) or fibrils containing  $\text{Cu}^{2+}$  (the end point). Nevertheless, it is important to demonstrate that fibrils containing  $\text{Cu}^{2+}$ , but assembled in the absence of glycerol, exhibit  $\text{Cu}^{2+}$  EPR spectra and temperature dependences identical to those of  $\text{Cu}^{2+}$ -containing fibrils formed in the presence of glycerol. Figure 4 shows that the EPR spectrum of  $\text{Cu}^{2+}$ -containing fibrils assembled without glycerol is very similar to that for  $\text{Cu}^{2+}$ -containing fibrils assembled in the presence of glycerol. For fibrils assembled with  $\text{Cu}^{2+}$  but without glycerol, the  $\text{Cu}^{2+}$   $g_{\parallel}$  value is 2.25 and  $A_{\parallel}$  is  $174 \pm 2$  G. Like  $\text{Cu}^{2+}$  bound to fibrils assembled in the presence of glycerol, these fibrils display a normal Curie temperature dependence of the  $\text{Cu}^{2+}$  EPR signal (Figure 4, inset). Thus, although glycerol affects the random coil to  $\beta$ -sheet transition rate of  $\text{A}\beta$ ,<sup>36</sup> it has little effect on the EPR properties of  $\text{Cu}^{2+}$  bound to  $\text{A}\beta$  fibrils.

The temperature dependence of the EPR signal of  $\text{Cu}^{2+}$  bound to soluble  $\text{A}\beta$  can be interpreted in several ways. One possibility is that our samples contain both  $\text{Cu}^{2+}$  and  $\text{Zn}^{2+}$  and form an imidazolate-bridged Cu, Zn binuclear center in which the  $\text{Cu}^{2+}$  behaves like a mononuclear center. This explanation would require that samples contain high levels of contaminating  $\text{Zn}^{2+}$  prior to the addition of  $\text{Cu}^{2+}$  and that a significant fraction of added  $\text{Cu}^{2+}$  be detected as free  $\text{Cu}^{2+}$ . In Tris buffers, both bound and unbound  $\text{Cu}^{2+}$  ions are detectable. We observe no free  $\text{Cu}^{2+}$  when a stoichiometric amount of  $\text{Cu}^{2+}$  is added to soluble  $\text{A}\beta$ . It has been demonstrated that  $\text{Cu}^{2+}$  can displace  $\text{Zn}^{2+}$ ,<sup>7</sup> so  $\text{Cu}^{2+}$  should replace  $\text{Zn}^{2+}$  in our samples if  $\text{Zn}^{2+}$  is bound to the  $\text{Cu}^{2+}$  site. These observations rule out a situation in which  $\text{Cu}^{2+}$  sites are occupied by  $\text{Zn}^{2+}$  prior to the addition of exogenous  $\text{Cu}^{2+}$  to  $\text{A}\beta$ .

A second possibility is that both a Type 2  $\text{Cu}^{2+}$  site, observable at temperatures below 60 K, and a binuclear  $\text{Cu}^{2+}$  site, which is not observable at temperatures below 60 K, exist in soluble  $\text{A}\beta$ . If this situation is applicable, addition of  $\text{Cu}^{2+}$  to soluble  $\text{A}\beta$  should load both the binuclear site and the Type 2 site, resulting in only a fraction of the added  $\text{Cu}^{2+}$  (bound in the Type 2 site) being observed in our spectra. Quantification of the  $\text{Cu}^{2+}$  concentration by double integration of the  $\text{Cu}^{2+}$  EPR signal for  $\text{Cu}^{2+}$  bound to soluble  $\text{A}\beta$  typically deviates by less than 10% from the expected concentration of added  $\text{Cu}^{2+}$  on the basis of comparison to a calibration curve,<sup>37</sup> making the existence of both a Type 2 and a binuclear site in soluble  $\text{A}\beta$  unlikely.

A final possibility is that, at stoichiometric ratios of  $\text{Cu}^{2+}$  and  $\text{A}\beta$ ,  $\text{Cu}^{2+}$  is bound in a mononuclear site and is not antiferromagnetically coupled through a histidine bridge to another  $\text{Cu}^{2+}$  ion. The EPR spectrum for stoichiometric ratios of  $\text{Cu}^{2+}$  bound to soluble  $\text{A}\beta(1-40)$  broadens as the temperature increases. The same trend is observed for spectra of  $\text{Cu}^{2+}$  incorporated into fibrillar  $\text{A}\beta$ . Observation of the broadened EPR spectrum for  $\text{Cu}^{2+}$  with soluble  $\text{A}\beta(1-28)$  as reported by Curtain et al. might be a function of the temperature (110 K) at which the spectrum was collected, rather than evidence for the existence of antiferromagnetically exchange-coupled  $\text{Cu}^{2+}$  ions in  $\text{A}\beta$ .

Our results have implications for the formation and global structure of fibrils assembled in the presence of  $\text{Cu}^{2+}$ . The ligand donor atoms to  $\text{Cu}^{2+}$  in soluble and fibrillar  $\text{A}\beta(1-40)$  are the same, potentially indicating that the  $\text{Cu}^{2+}$  ligands also are the same. A mechanism for metal-induced  $\text{A}\beta$  aggregation involving imidazolate-bridged binuclear  $\text{Cu}^{2+}$  centers is not supported by our results, even though such a model might explain the increased rate of  $\text{A}\beta$  aggregation observed in the presence of metal ions.<sup>3,5,38</sup> Similarly,  $\text{A}\beta(1-40)$  fibrils assembled in the presence of  $\text{Cu}^{2+}$  do not contain binuclear  $\text{Cu}^{2+}$  sites in which  $\text{Cu}^{2+}$  ions are antiferromagnetically coupled, even though such an arrangement might be possible given the 5 Å interstrand distance in parallel  $\beta$ -sheets. Finally, the one  $\text{Cu}^{2+}$  ion per peptide ratio and 3N1O coordination environment for  $\text{Cu}^{2+}$  in fibrils exclude a model for  $\text{A}\beta$  fibrils in which one  $\text{Cu}^{2+}$  ion is ligated to four histidine residues from multiple peptides to form cross-links between  $\beta$ -sheets as has been proposed for  $\text{Zn}^{2+}$ .<sup>5,15,39</sup>

**Acknowledgment.** This research was supported by the American Health Assistance Foundation through an Alzheimer's Disease Research Pilot Project Award (A2003-227). L.J.K. was the recipient of a UMBC Provost Undergraduate Research Award. We thank Dr. L. C. Patino (MSU) for ICP-MS experiments and Dr. R. Naumann (UMB) for EM images. Critical reading of the manuscript by Dr. David H. Stewart is gratefully acknowledged.

JA0488028

(37) For example, in Figure 1, the calculated  $\text{Cu}^{2+}$  concentration for  $\text{Cu}^{2+}$  bound to soluble  $\text{A}\beta(1-40)$  is 54  $\mu\text{M}$ , whereas the expected value is 50  $\mu\text{M}$ . Microwave power saturation data for  $\text{Cu}^{2+}$  bound to  $\text{A}\beta$  revealed that the power saturation behavior differed from that for the  $\text{Cu}^{2+}$  standards, even though all samples were in the same buffer. None of the spectra was collected at saturating powers. For quantification purposes, double integrations of baseline-corrected spectra for  $\text{Cu}^{2+}$  bound to soluble  $\text{A}\beta$  were corrected to account for the  $P_{1/2}$  difference.

(38) Atwood, C. S.; Moir, R. D.; Huang, X.; Scarpa, R. C.; Bacarra, N. M. E.; Romano, D. M.; Hartshorn, M. A.; Tanzi, R. E.; Bush, A. I. *J. Biol. Chem.* **1998**, *273*, 12817.

(39) Lynn, D. G.; Meredith, S. C. *J. Struct. Biol.* **2000**, *130*, 153.

(36) Yang, D. S.; Yip, C. M.; Huang, T. H.; Chakrabarty, A.; Fraser, P. E. *J. Biol. Chem.* **1999**, *274*, 32970.